COMPUTATIONAL METHOD FOR POWER LINE MAGNETIC FIELD EVALUATION

Santi Tofani and Giovanni d'Amore

LABORATORIO DI SANITA' PUBBLICA - SEZIONE FISICA , 10015 IVREA (TO), ITALY

and

Giancarlo Bonazzola and Giovanni Fiandino

DIPARTIMENTO DI FISICA SPERIMENTALE, UNIVERSITA' DI TORINO , ITALY

ABSTRACT - The paper reports a model for the power line magnetic field evaluation. The obtained results for three different power lines (380 kV double circuit, 380 kV single circuit, 220 kV double circuit) was validated with measurement data. Calculated and corresponding measured data were found in good agreement. The influence of geometrical and electrical power line parameters, such as the spatial configuration of the conductors and line phase sequences, is evaluated and discussed. Data on the influence of adjacent line span on the field are also reported.
The method can be used for prediction of human exposure in epidemiological studies.

INTRODUCTION

In the past years some papers [Wertheimer and Leeper, 79-82; Tomenius, 86; Savitz, 88] have proposed a possible correlation between exposure to low-level magnetic field generated by transmission lines and the increase of cancer and leukaemia risk.
A more accurate way of assessing magnetic field human exposure has been considered necessary by the International Agency for Research on Cancer in order to better understand the results of epidemiological studies [Ad Hoc Working Group, 90]. Computational methods allowing an accurate evaluation of the magnetic field pattern around transmission lines, can be of great help in the human exposure assessment.
Other authors [Deno, 76; Hart and Marino, 77; CIGRE', 80; Olsen and Pankaskie, 83; Olsen and Jaffa, 84; Olsen and Rouseff, 85] have reported theoretical analyses of transmission line magnetic fields. These analyses are based on several assumptions to simplify the calculation procedure such as conductors being parallel to the ground, a flat earth and two dimensional space.
Our paper regards a calculation method to be used for the evaluation of magnetic field emitted by transmission lines. The method takes also in account for the real conductor configuration, geometrical characteristic of the line and earth orography.
Comparison between calculated and measured magnetic field values for different kinds of transmission lines is also reported.

CALCULATION METHOD

In a transmission line span the conductors describe a catenary curve Γ which is represented, in the conductor plane, by the following function:

$$Y(x) = \frac{Y_v}{2}\left(e^{x/Y_v}+e^{-x/Y_v}\right) = Y_v \cosh\frac{x}{Y_v} \qquad (1)$$

where we have considered a reference system with y axis coincident with catenary axis and x axis at a

distance Y_V from the catenary vertex (see fig.1).
The magnetic field B generated by a generic line conductor which describes a Γ curve at a P point in space is given, using the Ampere-Laplace law, by:

$$\vec{B} = \mu_o \int_\Gamma I \frac{d\vec{l} \times \vec{r}}{4\pi r^3} \qquad (2)$$

where I is the current which flows in the line conductor element dl, r is the distance between the dl element and the P point and μ_0 is the vacuum permeability.
In order to obtain data of the three field orthogonal components, we have solved the integral of eq. (2) by using the numerical Simpson method [Gerald, 70] for the integral corresponding to the three orthogonal components of vector dl×r.

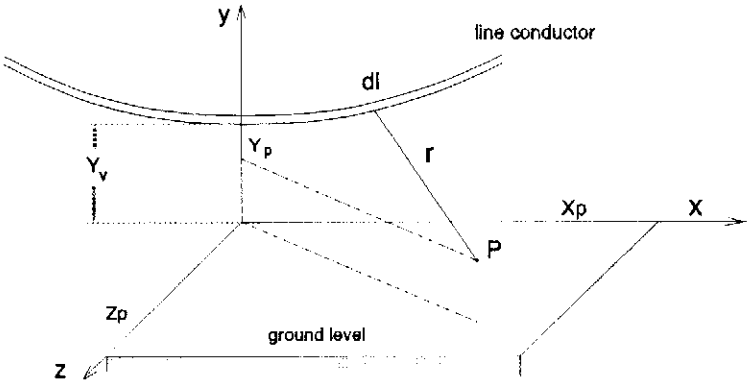

Fig.1 The adopted orthogonal reference system.

If we assume that the conductor plane is the y-x plane (see fig. 1), the z component of dl is zero. So, we can write the three components of differential contribution (dB) to B field as:

$$dB_x = \mu_o I \frac{Z_p\, dy}{4\pi r^3} \qquad (3a)$$

$$dB_y = -\mu_o I \frac{Z_p\, dx}{4\pi r^3} \qquad (3b)$$

$$dB_z = \mu_o I \frac{[(y-Y_p)\, dx - (x-X_p)\, dy]}{4\pi r^3} \qquad (3c)$$

where dy and dx are the dl components in the y and x direction respectively and Z_P, Y_P and X_P are the three orthogonal P coordinates in the reference system considered.
By differentiation of function reported in eq. (1) we obtain:

$$dy = \sinh\frac{x}{Y_v}\,dx \tag{4}$$

Substituting dy contained in equations (3a) and (3c) with expression obtained in eq. (4), the three components of differential magnetic field (dB) can be written as:

$$dB_x = \frac{\mu_o I Z_p}{4\pi r^3}\sinh\left(\frac{x}{Y_v}\right)dx \tag{5a}$$

$$dB_y = \frac{\mu_o I Z_p}{4\pi r^3}\,dx \tag{5b}$$

$$dB_z = \frac{\mu_o I}{4\pi r^3}\left[\left(Y_v\cosh\left(\frac{x}{Y_v}\right) - Y_p\right) - (x - X_p)\sinh\left(\frac{x}{Y_v}\right)\right]dx \tag{5c}$$

By simple algebraic calculations and using the expression (1), we can express the distance r as a function of only x variable:

$$r = \sqrt{(x-X_p)^2 + Z_p^2 + \left(Y_v\cosh\left(\frac{x}{Y_p}\right) - Y_p\right)^2} \tag{6}$$

Once we have expressed r as a function of only x, the equations (5a), (5b), (5c) become:

$$dB_x = \frac{\mu_o I}{4\pi}\,\frac{\sinh\left(\frac{x}{Y_v}\right)}{\left[(x-X_p)^2 + Z_p^2 + \left(Y_v\cosh\left(\frac{x}{Y_v}\right) - Y_p\right)^2\right]^{3/2}}\,dx \tag{7a}$$

$$dB_y = \frac{\mu_o I}{4\pi}\,\frac{dx}{\left[(x-X_p)^2 + Z_p^2 + \left(Y_v\cosh\frac{x}{Y_p} - Y_p\right)^2\right]^{3/2}} \tag{7b}$$

$$dB_z = \frac{\mu_o I}{4\pi}\,\frac{\left[\left(Y_v\cosh\left(\frac{x}{Y_v}\right) - Y_p\right) - (x-X_p)\sinh\left(\frac{x}{Y_v}\right)\right]}{\left[(x-X_p)^2 + Z_p^2 + \left(Y_v\cosh\left(\frac{x}{Y_p}\right) - Y_p\right)^2\right]^{3/2}}\,dx \tag{7c}$$

The result of the integration on the catenary is a magnetic field B whose j-th orthogonal component is:

$$B_j = A_j\cos(\omega t + \phi_j) \tag{8}$$

where A_j is the amplitude of the field and ϕ_j is its phase.
The total magnetic field generated by the transmission line has to be evaluated considering the contributions of the single conductors and the interferences resulted from the superposition of the fields generated by the several conductors which constitute the line.
The j-th orthogonal component of the total B field (B_{totj}) is given:

$$B_{totj} = A_{totj}\cos(\omega t + \phi_{totj}) \tag{9}$$

where:

$$\phi_{totj} = \arctan\left[\frac{\sum_{i=1}^{3} A_{ji}\sin\varphi_{ji}}{\sum_{i=1}^{3} A_{ji}\cos\varphi_{ji}}\right] \qquad (10a)$$

$$A_{totj} = \sqrt{\sum_{i=1}^{3} A_{ji}^2 - \frac{1}{2}\sum_{i}\sum_{k} A_{ji}A_{jk}} \quad , \; i \neq k \qquad (10b)$$

In the above reported expressions we have represented with A_{ji} and ϕ_{ji} the amplitude and the phase respectively of the j-th component of the field produced by the i-th conductor. In writing the equation (10b) we assume that the difference between the phases relative to the conductors is equal to 120°.
Equations (10a) and (10b) can be applied also to a double circuit transmission line, which is constituted (see fig. 2) by three couples of phased conductors (on the whole six conductors). For this type of line i index refers to each couple of phased conductors and so A_{ji} have to be equal to the sum of the B_j components produced by the single conductors of the i-th couple.
The earth influence on field pattern can be evaluated using the image method, which considers the contribution to B_{tot} due to image currents placed under the ground. These image currents must be chosen such that the following boundary conditions at air-ground interface are satisfied:

$$B_{1n} = B_{2n} \qquad (11a)$$

$$\frac{B_{1t}}{\mu_o} = \frac{B_{2t}}{\mu_1} + J_S \qquad (11b)$$

where B_{1n} and B_{1t} are respectively the normal and tangential B components in the air and B_{2n} and B_{2t} are respectively the normal and tangential B components in the earth, J_S is a surface current flowing upon the interface, and μ_0 and μ_1 are respectively the air and the ground permeability.
As the earth has a finite conductivity ($\sigma = 10^{-1} \div 10^{-3}$ mhos/m) J_S cannot exists on the interface and the boundary condition for tangential component of B field (eq. 11b) becomes:

$$\frac{B_{1t}}{\mu_o} = \frac{B_{2t}}{\mu_1} \qquad (11c)$$

By using the above reported Ampere-Laplace law, see eq. (2), and considering the geometric parameters shown in the scheme of figure 3, the tangential and normal components of B field generated by a current with a J density can be given, in a P point on the ground (see fig. 3), by the following expressions:

$$B_{1n} = \frac{\mu_0}{4\pi} JA \int_\Gamma \frac{x_o dl}{(x_o^2 + y_1^2)^{3/2}}; \qquad B_{1t} = \frac{\mu_0}{4\pi} JA \int_\Gamma \frac{x_o dl}{(x_o^2 + y_1^2)^{3/2}}; \qquad (12)$$

where A is the area of conductor section, and x_0 and y_1 are the projection of position vector r respectively

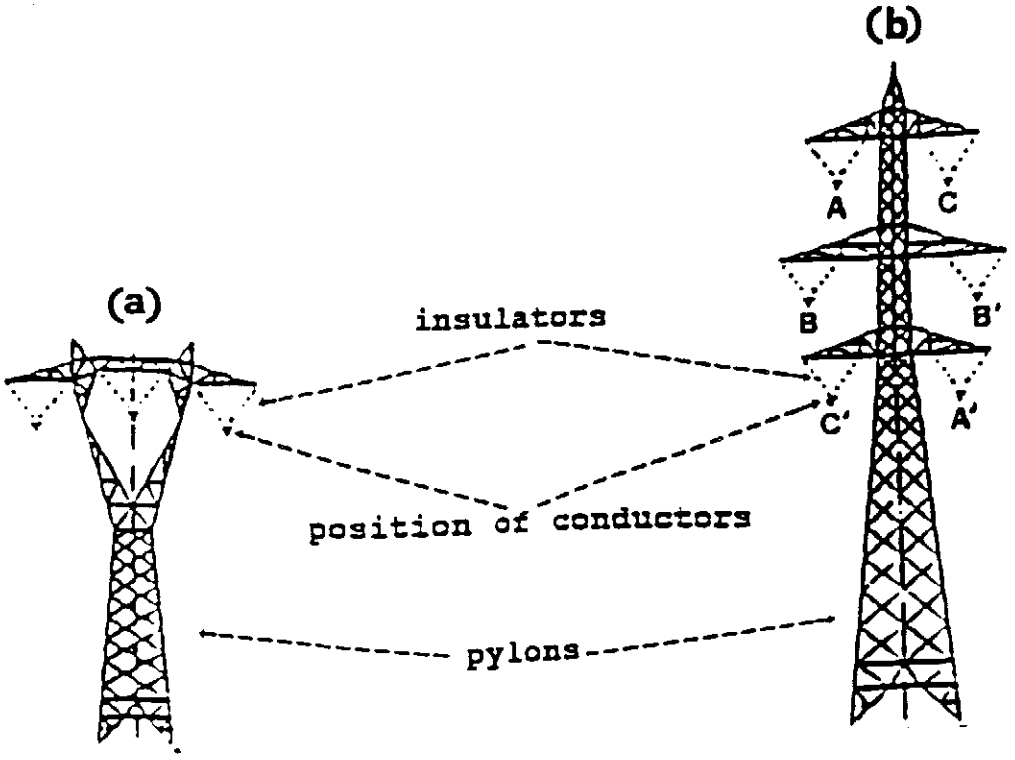

Fig.2 The basic structure of: (a) a single circuit 3-phase line; (b) a double circuit 3-phase line.
In the figure (b), A-A', B-B' and C-C' letters indicate the three couples of conductors in which current with the same phase flows. In this figure is represented one of the possible configurations of phased conductors, which is named crossed phase configuration.

on x-z plane and y-z plane. We note that both x_0 and y_1 are dependent of l integration variable.

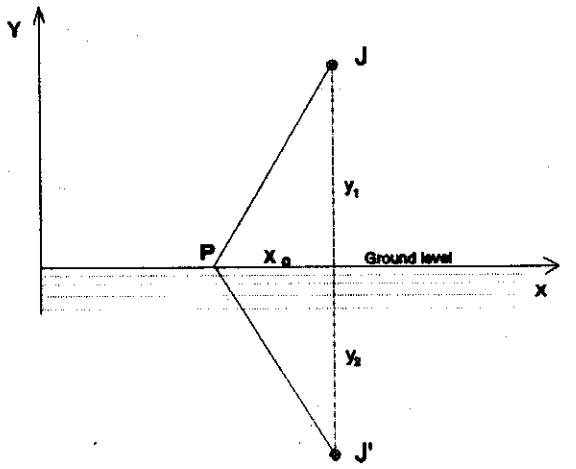

Fig.3 Cross section of real (J current density) and image (J' current density) conductors placed in opposite sides of the ground level.

If we express the B tangential and normal components by the equations (12), the boundary conditions (11a) and (11c) can be written as:

$$\frac{\mu_0}{4\pi} JA\alpha - \frac{\mu_0}{4\pi} J'A\beta = \frac{\mu_1}{4\pi} J''A\alpha \qquad (13a)$$

$$\frac{JA}{4\pi}\gamma - \frac{J'A}{4\pi}\epsilon = \frac{J''A}{4\pi}\gamma \qquad (13b)$$

where J' is the image current and J'' is a current density distributed in the space as J, generating the B field (B_2) under the ground; the coefficients α, β, γ and ϵ are respectively given by:

$$\alpha = \int_\Gamma \frac{x_o dl}{(x_o^2+y_1^2)^{3/2}}; \qquad \beta = \int_\Gamma \frac{x_o dl}{(x_o^2+y_2^2)^{3/2}};$$

$$\gamma = \int_\Gamma \frac{y_1 dl}{(x_o^2+y_1^2)^{3/2}}; \qquad \epsilon = \int_\Gamma \frac{y_2 dl}{(x_o^2+y_2^2)^{3/2}};$$

The simultaneous solution of equations 13a and 13b gives the following relation between image current density J' and real current density J:

$$J' = \frac{\mu_o - \mu_1}{\mu_o \frac{\beta}{\alpha} + \mu_1 \frac{\epsilon}{\gamma}} J \qquad (14)$$

As immediate consequence of equation (14) it results that J' = 0 if $\mu_0 = \mu_1$. So if we assume that air permeability is approximately equal to ground permeability ($\mu_0 \approx \mu_1$) we can neglect image currents in the

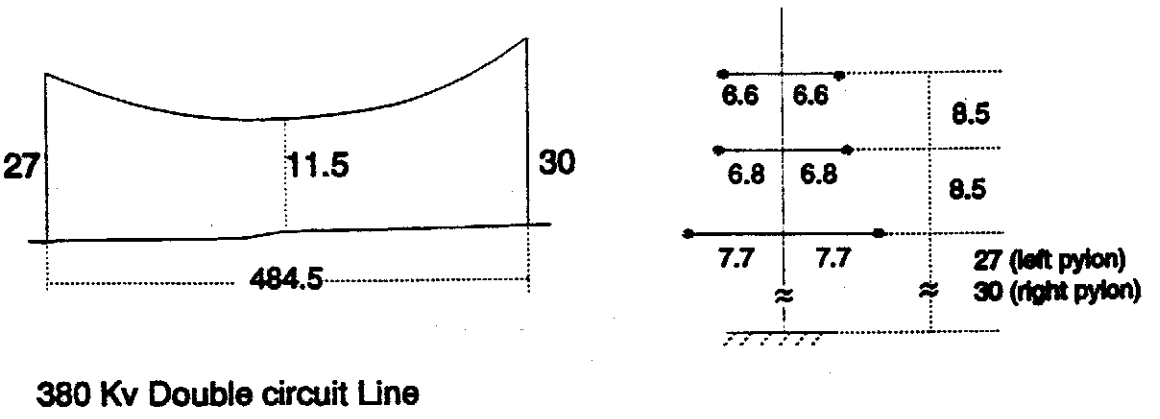

380 Kv Double circuit Line

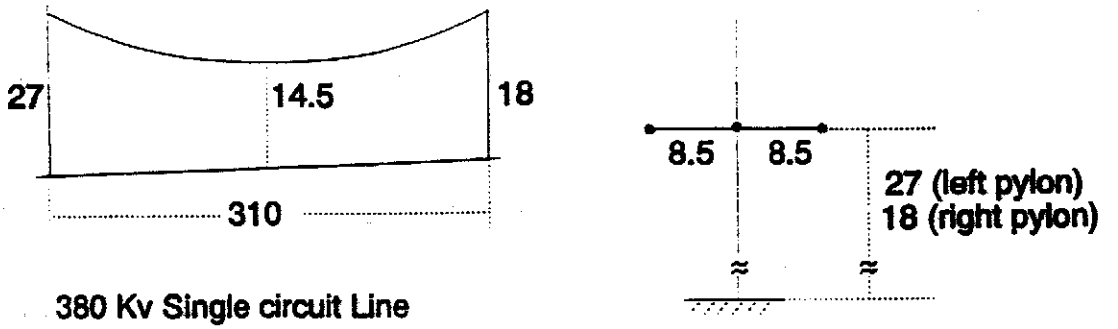

380 Kv Single circuit Line

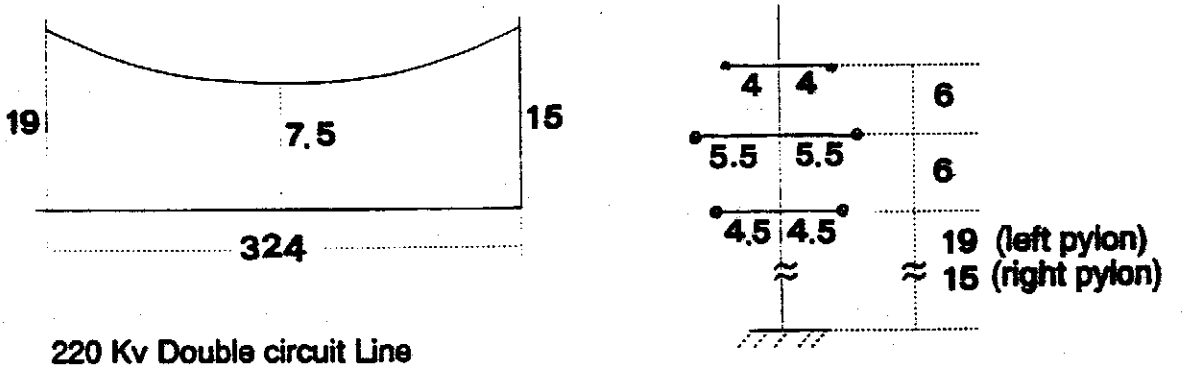

220 Kv Double circuit Line

Fig.4 The geometric characteristics of line spans and pylons relative to the three types of transmission lines considered in this work. All the distances reported in this figure are expressed in meters.

power line magnetic fields calculation procedure.
The above reported computational procedure has been applied to three different transmission lines. The lines taken in consideration were: a) 380 kV double circuit line, b) 380 kV single circuit line, c) 220 kV double circuit line. In figure 4 we have reported the geometric characteristics of pylons and spans relative to the three type of line that we have considered in this paper.
Current flowing in the conductors was measured by National Electricity Generating Board (ENEL) at the station which receive the high voltage electricity and redistribute it at lower voltages. Calculation of the current variation due to the electric characteristics of the line was used, together with the measured values, to assess the current flowing in the considered line span.
Using the calculation procedure, the per cent current variation is found to be about 10% for a line segment length of 100 km.
The calculated B values have been compared with measurement data. The measurements were performed using broad-band and narrow-band measurement systems. The use of these systems and the obtained results are reported in detail in [Tofani and al.].

RESULTS

Comparison between magnetic field profiles calculated assuming rectilinear and catenary conductor distribution is reported in figure 5. We have used two different rectilinear conductors distributions. In the first one (distribution a) the conductors are approximated to straight lines crossing the two points in which each conductor is connected to the two pylons of a span, while in the second distribution (distribution b) the conductors are approximated by straight lines, parallel to the ground and crossing the point of intersection between the conductors itself and the test plane (perpendiculary to the line). This last approximation is widely used [Deno, 1976], while the first one can be used when the pilons heights are the only data known with accuracy. Figure 5 shows that the approximation of catenary conductors with rectilinear conductors can lead to a sensible disagreement in the B evaluation.

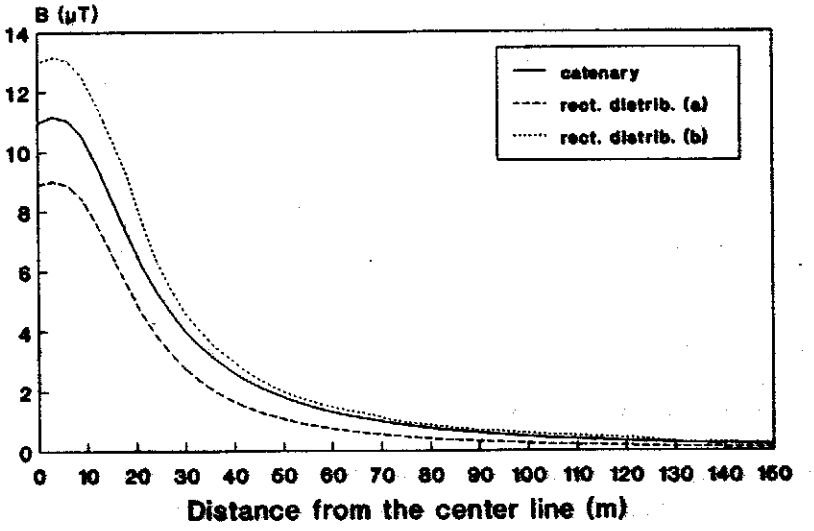

Fig.5 Magnetic field magnitudes calculated, 1.5 m above the ground, considering catenary conductors and rectilinear conductors (distributions (a) and (b)) with a load current of 1000 A. These profiles refer to a 380 kV, 50 Hz double circuit line. The minimum height of conductors is 13 m from the ground.

In the examined case of rectilinear distribution (distribution a, see fig.5) the deviation from the catenary distribution is on the order of -30% up to a distance of about 30 meters from the center line and becomes greater as the distance increases and B values decrease reaching about -50 % at a distance of 150 m, and

vanishing for a further increase of the distance; in the case of the second rectilinear distribution (distribution b, see fig.5) the deviation is on the order of 16% up to a distance of about 30 meters from the center line and vanish for a further increase of the distance. The reported differences due to modeling the line with linear conductors instead of catenary one can increase when adiacent spans taking angles different 180° are concerns.

The influence of the line phase arrangements in the magnetic field profiles for a double circuit power line can be seen in Figure 6.

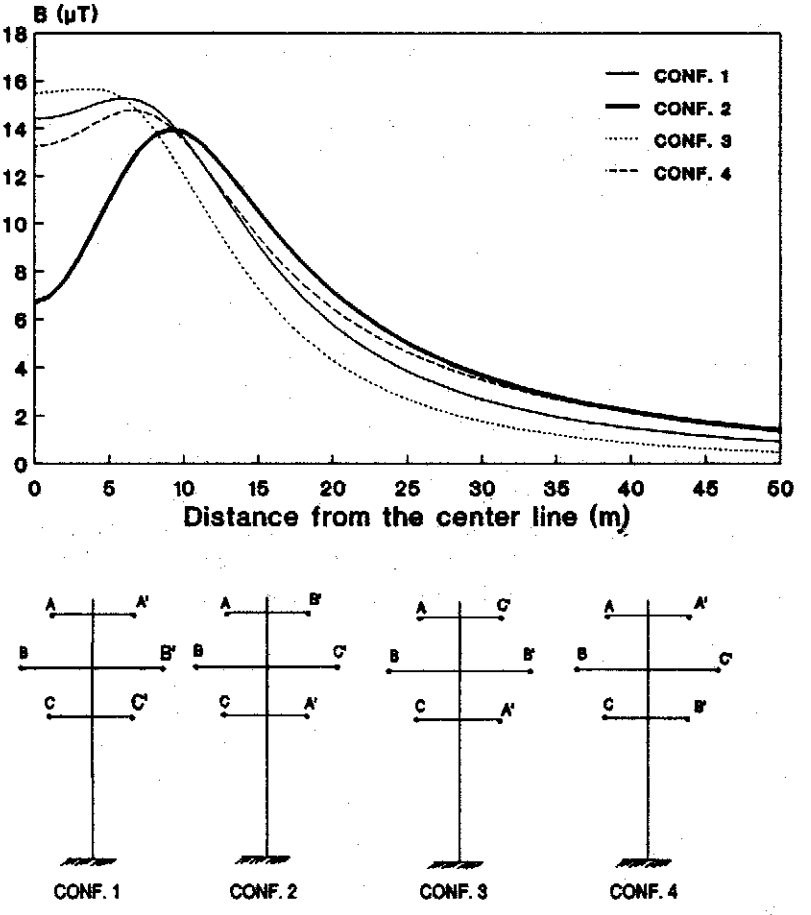

Fig.6 Profiles of magnetic field magnitudes calculated at a 1.5m above ground, under a 380 kV, 50 Hz double circuit line for four different phase arrangements, illustrated in the lower part of this figure (conf.1÷4). The minimum line height is 12 m. The line loading is 1000 A.

The Figure 6 reports B values versus distance for four different phase configurations. Configuration 3, also named configuration with crossed phases, gives the lowest B values further than about seven meters from the center line. The highest values are given by the configuration 1 further than about 10 meters from the center line.

Furthermore from figure 6 we can see that the per cent differences between B values corresponding to the configuration 3 and those of configuration 1 vary from 30 % at a distance of 15 m from the center line to 70 % at a distance of 50 m from the center line.

Under the line the differences are amplified and the configuration 1 gives the lowest field, while the configuration 3 gives the highest one.

Comparison between calculated and measured B values are reported in figure 7. The measurements were made at the middlespan level in a plane perpendicular to the line, where 380 kV single circuit line and 220

(a)

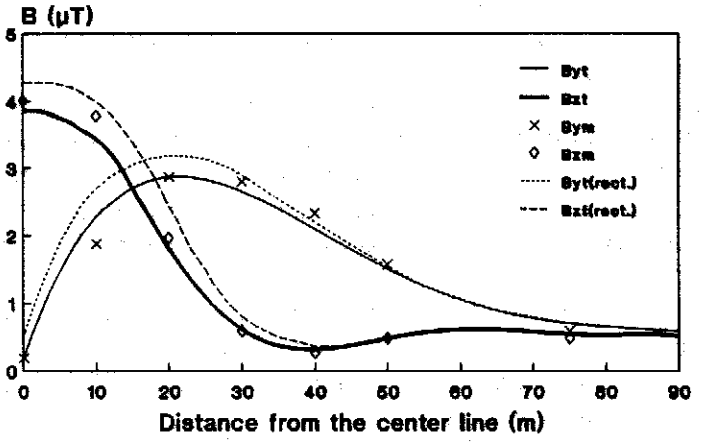

(b)

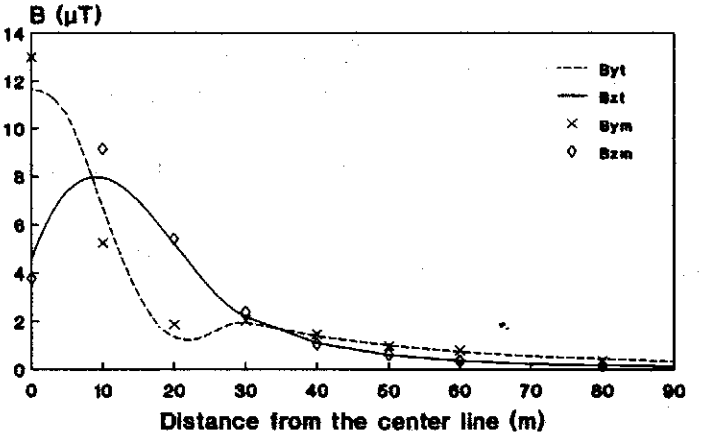

(c)

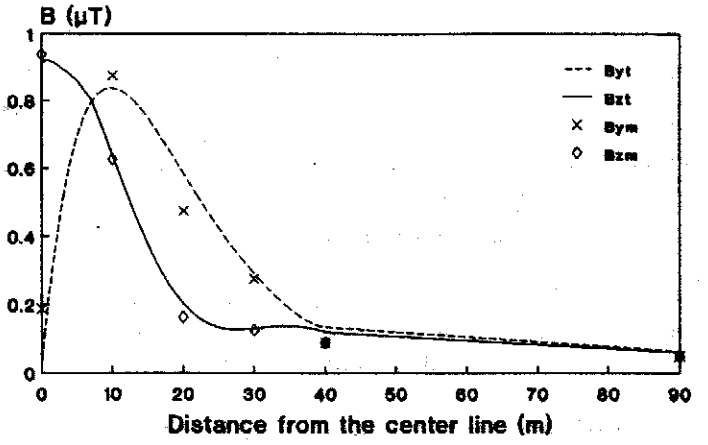

Fig.7 Theoretical (lines —— and ——) and experimental (symbols ◇ and ×) profiles of two magnetic field components (B_y and B_z) calculated at a 1.5 m above ground, under: (a) 380 kV double circuit line, (b) 380 kV single circuit line, (c) 220 kV double circuit line. Byt and Bzt are the calculated B_y,B_z component, while Bym and Bzm are the respectively correspondent experimental components. Load current is 850 A for (a) transmission line 1160 A for (b) transmision line and about 100 A for 220 kV line. The catenary vertex of the lowest wire was at 12 m ((a) transmission line), 13 m ((b) transmission line) and 12 m ((c) transmission line) from the line. The additional theoretical data reported in (a), i.e. B_yt(rect.) and B_zt(rect.), refer to the assumption of rectilinear line conductors parallel to the ground and tangential to the minimum of line catenary.

kV double circuit line were considered, and at a distance of 124 m from the middlespan, where 380 kV double circuit line was considered.
Figure 7 doesn't report data regarding the Bx component because the values of this component are found to be negligible in respect to the other two orthogonal component values (By, Bz).
We observe that the used model gives results in a good agreement with the experimental data. The mean value of the differences between all the corresponding theoretical and experimental data is resulted to be about 9.5 %. This value is very close to the accuracy (8%) evaluated for the used measurement systems [Tofani and al.].
The obtained agreement can be very satisfactory considering also that the used measurement systems don't take in account for the accuracy in the positioning of the meter.
If we compare theoretical data, obtained assuming rectilinear conductors (B_yt(rect.) and B_xt(rect.)) with the experimental ones, we find a mean difference of 20%.
The decrement of the accuracy between experimental and theoretical data going from catenary assumption to the rectilinear conductors approximation justify the added effort in increasing the mathematical complexity needed for the catenary approach.
So far we have calculated the B field considering only one line span and neglecting the field generated by the adjacent spans. However, there are regions in space in which can be of interest to evaluate also the B field emitted by closer adjacent span, and to compare it with the B field calculated considering only one span.
For example we can examine the case illustrated in figure 8, where are represented two adjacent spans S_1 and S_2 which form an angle $\vartheta = 150°$, with vertex in the common pylon P_c.

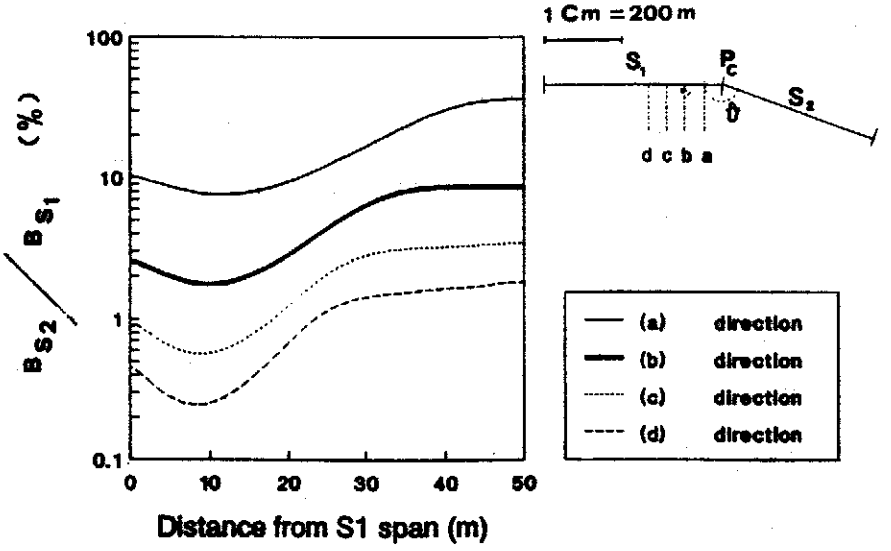

Fig.8 Percentage ratio between the B field produced by S_2 line span (B_{S2}) and that produced by S_1 line span (B_{S1}) versus distance from the center of S_1 span. a, b, c, and d are the four different perpendicular directions located respectively at distances of 50, 100, 150, 200 m from the common pylon Pc.

The "a", "b", "c" and "d" lines represent the directions, located respectively at distances of 50, 100, 150, 200 m from the common pylon Pc, along which we have calculated both the B field emitted by only S_1 span (B_{S1}) and the B field emitted by only S_2 span (B_{S2}).
Always in figure 8 is shown the comparison between B_{S1} and B_{S2} fields in the "a", "b", "c" and "d" directions up to a distance of 50 m from the S_1 line span.
We observe that in the considered case the magnetic field produced by S_2 span is negligible in respect to that produced by S_1 span ($B_{S2}/B_{S1} < 2\%$) along "c" and "d" directions. The B_{S2}/B_{S1} ratio is greater in "a" direction, where increases from 10% to 40 %, respectively at distances of 0 m and 50 m from the S_1 span. These results are strongly dependent from the angle (ϑ) formed by the two adjacent spans. When ϑ

kV double circuit line were considered, and at a distance of 124 m from the middlespan, where 380 kV double circuit line was considered.
Figure 7 doesn't report data regarding the Bx component because the values of this component are found to be negligible in respect to the other two orthogonal component values (By, Bz).
We observe that the used model gives results in a good agreement with the experimental data. The mean value of the differences between all the corresponding theoretical and experimental data is resulted to be about 9.5 %. This value is very close to the accuracy (8%) evaluated for the used measurement systems [Tofani and al.].
The obtained agreement can be very satisfactory considering also that the used measurement systems don't take in account for the accuracy in the positioning of the meter.
If we compare theoretical data, obtained assuming rectilinear conductors (B_yt(rect.) and B_zt(rect.)) with the experimental ones, we find a mean difference of 20%
The decrement of the accuracy between experimental and theoretical data going from catenary assumption to the rectilinear conductors approximation justify the added effort in increasing the mathematical complexity needed for the catenary approach.
So far we have calculated the B field considering only one line span and neglecting the field generated by the adjacent spans. However, there are regions in space in which can be of interest to evaluate also the B field emitted by closer adjacent span, and to compare it with the B field calculated considering only one span.
For example we can examine the case illustrated in figure 8, where are represented two adjacent spans S_1 and S_2 which form an angle $\vartheta = 150°$, with vertex in the common pylon P_c.

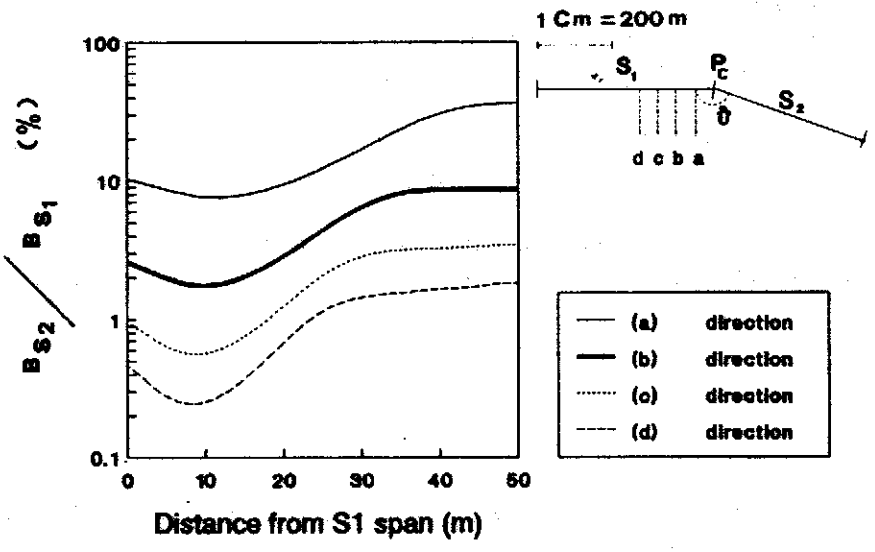

Fig.8 Percentage ratio between the B field produced by S_2 line span (B_{S2}) and that produced by S_1 line span (B_{S1}) versus distance from the center of S_1 span. a, b, c, and d are the four different perpendicular directions located respectively at distances of 50, 100, 150, 200 m from the common pylon Pc.

The "a", "b", "c" and "d" lines represent the directions, located respectively at distances of 50, 100, 150, 200 m from the common pylon Pc, along which we have calculated both the B field emitted by only S_1 span (B_{S1}) and the B field emitted by only S_2 span (B_{S2}).
Always in figure 8 is shown the comparison between B_{S1} and B_{S2} fields in the "a", "b", "c" and "d" directions up to a distance of 50 m from the S_1 line span.
We observe that in the considered case the magnetic field produced by S_2 span is negligible in respect to that produced by S_1 span ($B_{S2}/B_{S1} < 2\%$) along "c" and "d" directions. The B_{S2}/B_{S1} ratio is greater in "a" direction, where increases from 10% to 40 %, respectively at distances of 0 m and 50 m from the S_1 span. These results are strongly dependent from the angle (ϑ) formed by the two adjacent spans. When ϑ

increases B_{S2} values decrease in the considered directions.
So to determine the magnetic field along directions which are at a small distance (in the above examined case < 100 m) from the common pylon of two adjacent line spans, it is necessary to execute the above reported calculation procedure for both spans. Neglecting the contribution of one of the two spans to total B field, can give rise to large errors in the B amplitude estimation.

CONCLUSIONS

The reported transmission line model, elaborated considering also the actual spatial configuration of conductors (catenary) and the earth orography has given a good prediction of the magnetic field pattern under the line. Considering the measurement accuracy (not less than 8 %), the B calculated values are in good agreement with the measured ones (mean per cent difference equal to 9.5 %)
The more mathematical complexity needed for handling the method, in comparison with the previous methods, is justified by the accuracy improvement in the B estimation. In fact, in the examined lines, the differences between calculated and measured values decrease from 20 (using rectilinear conductors approximation) to 9.5 %.
The influence of geometrical and electrical line parameters, such as spatial configuration of the conductors and line phase sequences, in the B field has been analyzed.
Depending upon the type of the rectilinear conductors assumption used, the disagreement on the B estimate in comparison with the catenary data range, in the considered case, from 16 to 30 % up to a distance of 30 m from the center line, and can be of 50 % at 150 m.
At distances from the center line where the population exposure can be concerned (greater than 20 m from the center line), the influence of the phase sequences on B increases with the distance reaching 70 % at 50 m.
The model has been also used to evaluate the field contributions due to one of two adjacent line spans. In the considered case the contribution is significant only at distance closer than 100 m from the common pylon.
Considering the obtained results, the model can be of good help in the prediction of population exposure to power line magnetic field. This prediction can then be of interest for the interpretation of epidemiological results.

REFERENCES

Ad Hoc Working Group, (1990): Extremely low-frequency electric and magnetic fields and risk of human cancer. Bioelectromagnetics 11:91-99.

CIGRE (1980) : Electric and magnetic fields produced by transmission systems. CIGRE Report 36-01.

Deno DW, (1976) : Transmission line fields. IEEE Transactions on Power Appar. and Syst. 95:1600-1611

Gerald CF (1970) : Applied numerical analysis. Addison Wesley Ed.

Hart FX, Marino AA (1977) : Energy flux along high voltage transmission lines. IEEE Transactions on Biomed. Engineering 5:493-495, vol 24.

Olsen R.G., Pankaskie T.A. (1983) : On the Exact, Carson and Image Theories for Wires At or Above the Earth's Interface. IEEE Transactions on Power Apparatus and Systems 4:769-778, vol.102.

Olsen R.G., Jaffa K.C. (1984) : Electromagnetic Coupling from Power Lines and Magnetic Field Safety Analysis. IEEE Transactions on Power Apparatus and Systems 12:3595-3607, vol.103.

Olsen R.G., Rouseff D. (1985) : On the Wave Impedance for Power Lines. IEEE Transactions on Power Apparatus and Systems 3:711-717, vol.104.

Savitz DA, Wachtel H, Barnes FA, John EM, Tvrdik JG (1988) : Case-control study of childhood cancer and exposure to 60-Hz magnetic fields. American Journal of Epidemiology 1:21-38, vol.128.

Tofani S, d'Amore G, Tasso M : Accuracy in the assessment of magnetic field exposure from AC power lines. Submitted to IEEE Transactions on Electromagnetic Compatibility.

Tomenius L (1986) : 50-Hz electromagnetic environment and the incidence of childhood tumors in Stockholm County. Biolectromagnetics 7:191-207.

Wertheimer N, Leeper E (1979) : Electrical wiring configuration and childhood cancer. Am. J. Epidemiol. 109:273-284.

Wertheimer N, Leeper E (1982) : Adult cancer related to electrical wires near the home. Int. J. Epidemiol. 11:345-355.